

This article was downloaded by:

On: 25 January 2011

Access details: *Access Details: Free Access*

Publisher *Taylor & Francis*

Informa Ltd Registered in England and Wales Registered Number: 1072954 Registered office: Mortimer House, 37-41 Mortimer Street, London W1T 3JH, UK



## Separation Science and Technology

Publication details, including instructions for authors and subscription information:

<http://www.informaworld.com/smpp/title~content=t713708471>

### Analysis of Cobalt Extraction by DI-(2-Ethylhexyl) Phosphoric Acid in a Continuous Flow Stirred Tank with a Laser Capillary Spectro-Photometer

J. H. Bae<sup>a</sup>; L. L. Tavlarides<sup>a</sup>; M. Stamatovic<sup>b</sup>

<sup>a</sup> Department of Chemical Engineering and Materials Science, Syracuse University, Syracuse, NY <sup>b</sup> Institute for Technology of Nuclear and Other Mineral Raw Materials, Belgrade, Yugoslavia

**To cite this Article** Bae, J. H. , Tavlarides, L. L. and Stamatovic, M.(1988) 'Analysis of Cobalt Extraction by DI-(2-Ethylhexyl) Phosphoric Acid in a Continuous Flow Stirred Tank with a Laser Capillary Spectro-Photometer', *Separation Science and Technology*, 23: 12, 1453 – 1472

**To link to this Article:** DOI: 10.1080/01496398808075642

**URL:** <http://dx.doi.org/10.1080/01496398808075642>

PLEASE SCROLL DOWN FOR ARTICLE

Full terms and conditions of use: <http://www.informaworld.com/terms-and-conditions-of-access.pdf>

This article may be used for research, teaching and private study purposes. Any substantial or systematic reproduction, re-distribution, re-selling, loan or sub-licensing, systematic supply or distribution in any form to anyone is expressly forbidden.

The publisher does not give any warranty express or implied or make any representation that the contents will be complete or accurate or up to date. The accuracy of any instructions, formulae and drug doses should be independently verified with primary sources. The publisher shall not be liable for any loss, actions, claims, proceedings, demand or costs or damages whatsoever or howsoever caused arising directly or indirectly in connection with or arising out of the use of this material.

ANALYSIS OF COBALT EXTRACTION BY DI-(2-ETHYLHEXYL) PHOSPHORIC ACID  
IN A CONTINUOUS FLOW STIRRED TANK WITH A LASER CAPILLARY SPECTRO-  
PHOTOMETER

J. H. Bae and L. L. Tavlarides  
Department of Chemical Engineering  
and Materials Science, Syracuse  
University, Syracuse, NY 13244

M. Stamatovic  
Institute for Technology of  
Nuclear and Other Mineral  
Raw Materials, Belgrade,  
Yugoslavia

ABSTRACT

A laser capillary spectrophotometric technique is used to study and quantify the dispersed phase mixing effects on the performance of a one liter continuous flow reactor for the cobalt-di-(2-ethylhexyl) phosphoric acid extraction system. Bivariate distribution data show that, as the RPM increases, the drop size and drop concentrations change from widely to narrowly distributed, the former tending toward small drop sizes and the latter tending toward higher concentrations. Comparisons between the Monte Carlo simulation model predictions and experimental results, using an aqueous film reaction model, indicates that the simulation predicts the size distribution closely, the Sauter mean diameter within 10% error, and the extraction efficiency within 15% error.

INTRODUCTION

Dispersed phase mixing can have a significant effect on the reactor size required for a given conversion or on the conversion and the selectivity in a given reactor in complex chemical reaction systems with mass transfer resistances, especially for heterogeneous systems. Many investigators have reported the importance of the dispersed phase mixing [1-5] for these systems.

In order to develop a rational design of chemical reactors for liquid-liquid systems, it is necessary to account for the de-

tails of thermodynamic equilibria, chemical kinetics, mass transfer processes, and the effects of the dispersed phase mixing. As a step in that direction, thermodynamic equilibria and kinetic models of cobalt(II) nitrate-acetate buffer/di-(2-ethylhexyl) phosphoric acid (D2EHPA)-toluene system have already been developed in our laboratory [6,7]. By employing these equilibrium and kinetic models, reactor performance of a CFSTR was predicted by the Monte Carlo simulation based on the interval of quiescence method [7]. However, no comparison has been made to verify the simulation model.

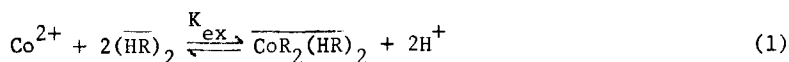
This study describes the application of the laser capillary spectrophotometric (LCS) technique developed by Bae and Tavlarides [8] to the cobalt-D2EHPA extraction system to quantify the dispersed mixing effects on the reactor performance for the goal of the optimum reactor design. The distribution of reactants and products due to the dispersed phase mixing as a result of variations in operating conditions are studied by generating bivariate (drop size and cobalt complex concentration) distribution data by the LCS technique. The kinetic model developed by Lee [6] is employed in the Monte Carlo simulation model to analyze the experimental results from the continuous flow stirred reactor (CFSTR). This investigation, thus, seeks to ascertain the impact of operation conditions on conversion and to confirm the validity of such a model to predict the performance of a CFSTR.

### Theory

The reaction chemistry (stoichiometry, thermodynamic equilibrium, and kinetics) must be understood before a reactor model for two-phase liquid-liquid reaction can be synthesized. Reaction chemistry for the cobalt(II)/D2EHPA extraction system and the Monte Carlo simulation technique incorporating mass transfer with reaction were previously discussed by Mukkavilli et al. [7]. In the section below, a brief description of this system and the Monte Carlo simulation are discussed.

### Reaction Chemistry and Interfacial Flux Extension

Komasawa et al. [9] studied the extraction of some divalent metals (Co, Ni, Cu) from the nitrate medium by D2EHPA. They found that the extraction reaction of cobalt can be represented by the following stoichiometric equation as long as the conversion of D2EHPA is less than 24%:



Here, the overbar represents the species existing in the organic phase and  $(\overline{\text{HR}})_2$  represents the dimeric form of D2EHPA. If the conversion ratio is greater than 24%, the polymerization of

organic metal complex would take place and Eq. (1) is no longer valid.

Lee [6] studied the reaction kinetics of cobalt(III) nitrate-acetate buffer/D2EHPA-toluene system using a modified Lewis cell. The experimental ranges of the kinetic study were  $[Co]_T$  (0.01-0.1M),  $[(HR)_2]_f$  (0.01-0.5M), and pH (3.16-5.02) at a temperature of 298°K. These experiments were designed such that the maximum conversion of D2EHPA is always less than 24% so as to minimize the polymerization of the cobalt complex. Hughes and Zhu [10] and Lee [6] proposed a reaction mechanism for the cobalt D2EHPA extraction based on an aqueous film reaction as outlined previously [7]. The model assumes dimerization of the chelation acid in the organic phase, partition of the monomer between the phases, dissociation of the chelation acid in the aqueous film, sequential addition of the anion to the cobalt ion in two steps, partition of the cobalt complex between phases and addition of the dimer to the cobalt complex in the organic phase. The rate expression derived when the rate determining step is the first addition of the anion to the cobalt ion becomes:

$$R_A = \frac{2k_1 K_A}{C_{H^+}} \left[ C_{Co^{2+}} C_{HR} - \frac{1}{K_{ex}} \frac{K_o P_{CoR_2}}{K_2 P_{HR}^2} \frac{C_{CoR_2} C_{H^+}^2}{C_{HR}} \right] \quad (2)$$

where,  $R_A$  is the rate of reaction of HR in the aqueous phase. Lee [6] used the limiting case of a pseudo first order reaction as discussed by Rod [21], i.e.,  $C_{Co^{2+}} = C_{CoO_6^{2+}}$  and  $C_{H^+}$  for  $0 \leq x \leq \delta$  and derived the interfacial flux of HR as follows:

$$J_{HR_i} = - \theta_1^{1/2} \left[ \frac{C_{Co^{2+}}}{C_{H^+}} \left( \frac{C_{HR_i}^2}{P_{HR}} - C_{HR_o}^2 \right) - \theta_2 \left( \frac{2C_{H^+} C_{CoR_2,1}}{P_{CoR_2}} + \frac{C_{H^+} C_{HR_i} D_{HR}}{P_{HR} D_{CoR_2}} \right) \ln \frac{C_{HR_i}}{C_{HR_o} P_{HR}} + \theta_2 \frac{C_{H^+} D_{HR}}{D_{CoR_2}} \left( \frac{C_{HR_i}}{P_{HR}} - C_{HR_o} \right) \right]^{1/2} \quad (3)$$

Here  $C_{HR_o}$  is the concentration of HR in the aqueous bulk phase for which an algebraic expression can be obtained [6]. The unknown

parameters  $\theta_1$ ,  $\theta_2$ , and  $P_{CoR_2}$  in eqn. (3) were determined by a non-linear least square analysis of experimental data [6] and have the values  $0.06 \text{ dm}^2/\text{sec}^2$ ,  $0.043$  and  $78.1$  respectively.

It is noted that conflicting views as to the location of reaction sites and mechanisms have been proposed by various investigators for this reaction system. The kinetic studies in our laboratory [6] with the stirred transfer reactor system, indicates that even under conditions where polymerization of the metal complex can be neglected, the extraction rates are substantially higher than pure mass transfer rates. This enhancement of the interphase transport rates is indicative of a film reaction mechanism and our justification for adoption of this aqueous film model. Eqn. (3) is employed in the simulation model to calculate the interphase mass transfer in the extractor modelling.

### Reactor Model

The Monte Carlo simulation model algorithm based on the interval of quiescence method [11-13] is used to predict the performance of a continuous flow stirred tank reactor for cobalt(II) nitrate-acetate buffer/D2EHPA-toluene system.

In the simulation technique, a representative fraction of the drop population is chosen and these drops are subjected to the influence of the reactor environment. For a CFSTR, the drops in the sample are allowed to undergo droplet events of entry, exit, breakage and coalescence. The evolution of the ensemble of drops to the final state is marked by successive sample events separated from each other by an interval of quiescence,  $t_{IQ}$ . This interval is computed by the Poisson arrival pattern analysis as follows:

$$t_{IQ} = \ln \chi / \sum_i f_i \quad (4)$$

where  $\chi$  is the uniform random number between 0 and 1, and  $f_i$  is the long range average frequency of  $i^{\text{th}}$  event. The long range frequencies of a drop are functions of the physical properties of the dispersion and the operating conditions of the CFSTR. During the interval of quiescence,  $t_{IQ}$ , smooth changes in concentrations of species are assumed to occur as a consequence of the mass flux due to concentration gradients and chemical reaction. The success of the simulation algorithm in predicting the performance of the extractor depends upon the validity of the drop rate models used. The event frequency functions which are used in this work are described elsewhere [11-13,15] and listed in Table 1. The breakage and coalescence frequencies are functions of physico-chemical properties of the system, but they also involve four unknown constants,  $C_1$ ,  $C_2$ ,  $C_3$  and  $C_4$ . The four constants used in this work have the same values as used by Bapat and Tavlarides [12]

TABLE 1  
Drop Event Frequencies [13-15]

| Name of Frequencies | Equations  |
|---------------------|--|
| Feed                | $f_f = V_d / \tau V_f$ (5)   |
| Exit                | $f_e = N / \tau$ (6)   |
| Breakage            | $f_b = \sum_{i=1}^N g(v_i)$ (7)  |
|                     | $g(v) = C_1 \frac{\epsilon^{1/3}}{(1+\phi)v^{2/9}} \exp[-C_2 \frac{\sigma(1+\phi)^2}{\rho_d \epsilon^{2/3} v^{5/9}}]$ (8)            |
| Coalescence         | $f_c = \frac{1}{2} \sum_{i=1}^N \sum_{\substack{j=1 \\ j \neq i}}^N F(v_i, v_j)$ (9)   |
|                     | $F(v_i, v_j) = h(v_i, v_j) \lambda(v_i, v_j)$ (10)   |
|                     | Collision rate:  |
|                     | $h(v, v') = C_3 \frac{\epsilon^{1/3}}{1+\phi} (v^{1/3} + v'^{1/3})(v^{2/9} + v'^{2/9})^{1/2}$ (11)                                   |
|                     | Collision frequency:   |
|                     | $\lambda(v, v') = \exp[-C_4 \frac{\mu_c \rho_c \epsilon}{\sigma^2 (1+\phi)^3} (\frac{v^{1/3} v'^{1/3}}{v^{1/3} + v'^{1/3}})^4]$ (12) |

The LCS technique employs a precision bore capillary of the order of droplet sizes present in liquid-liquid dispersions of interest. A sample stream of the dispersion is drawn from the mixing vessel by a vacuum pump. Figure 1 shows a flow diagram of the laser capillary spectrophotometer. The optical device is designed to measure drop size by the difference of light refraction between the two phases and to measure drop concentration by light absorbance of the cobalt complex (molar absorptivity = 168.5ℓ/moI-

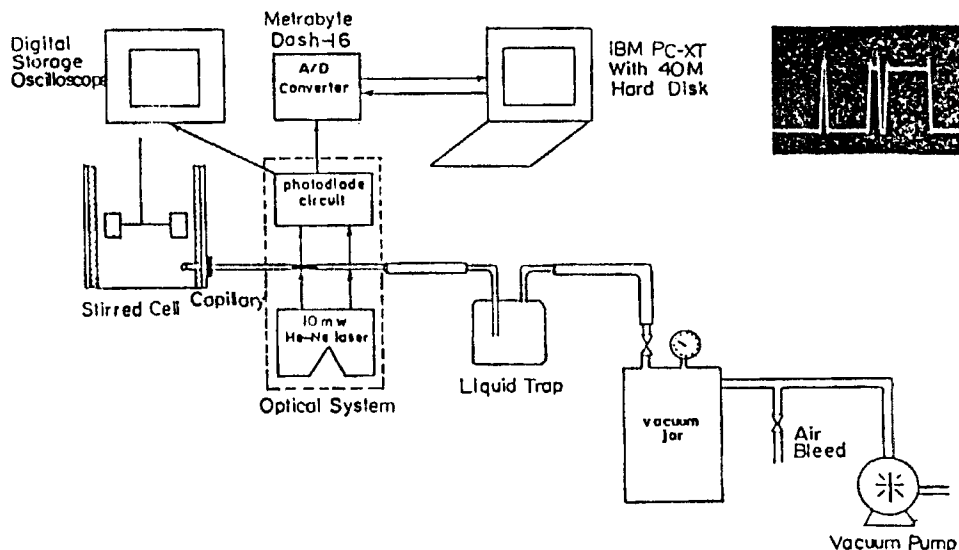


Figure 1: Laser Capillary Spectrophotometer Set-up

cm at 626 nm) in the drop. A He-Ne laser of 632.6 nm wavelength and 10 mW power (Spectra physics, model 102) is chosen for this purpose. The light beam from the laser is split into two beams which pass directly through the center of the capillary. The emergent beams from the capillary produce two series of rectangular pulses by the photodiodes coupled with photodiode circuits. An IBM PC with a Metrabyte DASH-16 A/D converter is used to sample and process the output signals from the photodiode circuit. These signals are also traced on an oscilloscope. Typical signals are shown in Figure 1 (insert). The width of each pulse is in proportion to the drop volume and the height of each pulse to the drop concentration. Details of this technique are given elsewhere [8, 19]. The reactor is also equipped to measure dispersed phase hold-up with an ultrasonic technique developed by Bonnet and Tavlarides (20).

### Chemicals

In these studies, feed solutions of 0.01M cobalt nitrate and 1M D2EHPA are used. This situation insures that the conversion of D2EHPA is less than 24%, and that the stoichiometric eqn. (1) is valid. The 1M D2EHPA solution is obtained by diluting commercial

D2EHPA, (purity: 97%) supplied by Albright and Wilson, Inc., with toluene without further purification. The cobalt nitrate solution is prepared with Fluka A.G. cobalt nitrate crystals dissolved in distilled water. Acetate buffer (NaOH-CH<sub>3</sub>COOH) solution is added to adjust the cobalt nitrate solution to pH = 4.0. All chemicals, except D2EHPA, which are used in this work are of reagent grade.

### Flow System and Operation

Figure 2 is a diagram of the experimental flow system. The continuous (aqueous) and the dispersed phase are fed into a 0.75ℓ stirred tank with equally spaced glass baffles. The input flow rates of each phase are measured with rotameters (FD,FC). The two phases are then mixed by the Rushton turbine agitator and leave through the exit stream to an effluent reservoir tank (ER). A vacuum pump (VP) is provided to evacuate the reactor as it is filled and to facilitate the withdrawal of samples through the dispersed phase coalescor (DC). The tank agitator is driven by a motor (SM) which is controlled to adjust the impeller rotational speed.

After steady state is reached (usually around 5 - 10 min), data acquisition is started. Capillary suction velocity is controlled by the vacuum pressure of the vacuum jar by an air bleed valve as shown in Figure 1. A capillary of 0.2mm diameter is employed in this work. After confirming the operation of the LCS technique (when two series of rectangular pulses are produced on the split screen oscilloscope), data acquisition is started by operating the A/D converter (DASH-16, Metrabyte Co). The calibration of drop concentration is carried out at the end of the experiment. Details of the operation procedure are described elsewhere [8,19].

## RESULTS AND DISCUSSION

### Experimental Results

Cobalt-D2EHPA extraction experiments were conducted to determine mixing effects on the reactor performance at conditions of  $\phi = 0.077 - 0.100$ ,  $\tau = 45 - 180s$ , and RPM - 250 - 400 (or  $\epsilon = 0.164 \text{ m}^2/\text{s}^3$  to  $0.673 \text{ m}^2/\text{s}^3$ ).

( $C_1 = 4.81 \times 10^{-3}$ ,  $C_2 = 8 \times 10^{-2}$ ,  $C_3 = 1.9 \times 10^{-3} \text{ cm}^{-3}$  and  $C_4 = 2 \times 10^8 \text{ cm}^{-2}$ ).

The turbulent characteristics in the reactor are assumed to be position invariant (homogeneous over the complete reactor volume) and characterized by the viscous energy dissipation per unit mass. The type of an event is decided by the probability of an event  $i$  occurring:

$$P_i = f_i / \sum f_i \quad (13)$$



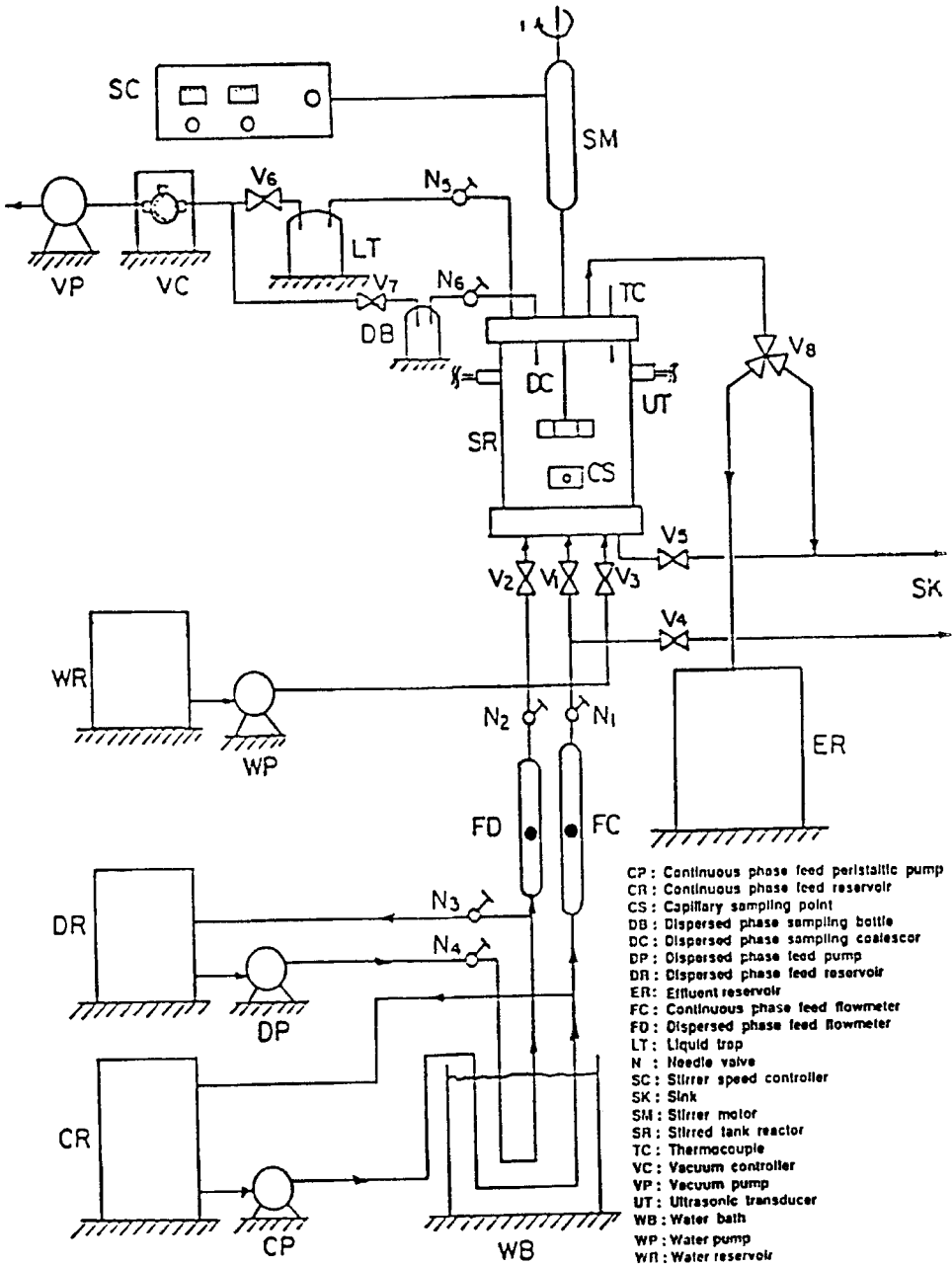


Figure 2: Experimental Flow System for a Continuous Flow Stirred Tank Reactor

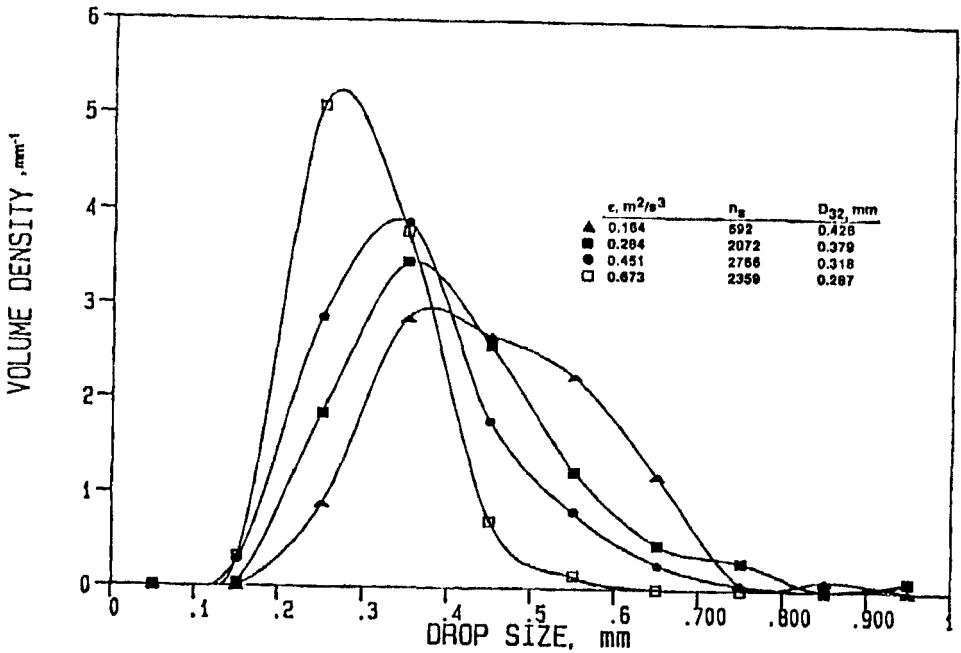


Figure 3: Influence of the Energy Dissipation Rate on Drop Size Distribution at  $\phi = 0.077$  and  $\tau = 45s$ .

Concentrations of all species of both phases including the extractant and cobalt complex in the organic phase are calculated for each drop by solving the corresponding species material balance equations:

$$\frac{\pi}{6} d_1^3 \frac{dC_{ij}^{(d)}}{dt} = \pi d_1^2 J_{ij} \quad (14)$$

$$v_c \frac{dC_j^{(c)}}{dt} = Q_c (C_{fj}^{(c)} - C_j^{(c)}) - \sum_{i=1}^N \pi d_i^2 J_{ij} \quad (15)$$

Here,  $C_{ij}^{(d)}$  represents the concentration of the  $j$ th species in the  $i$ th drop,  $J_{ij}$  is the interfacial flux of species  $j$  across the boundary of drop  $i$ , and  $C_{fj}^{(c)}$  and  $C_j^{(c)}$  are the continuous phase feed and product concentrations for species  $j$ . The flux for D2EHPA is

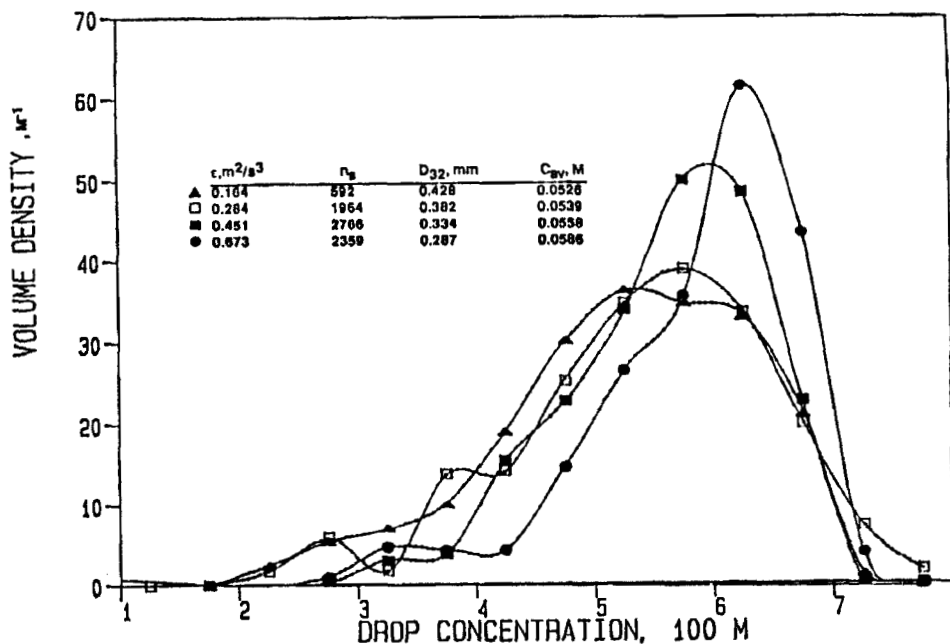


Figure 4: Influence of Energy Dissipation Rate on Drop Concentration Distribution at  $\phi = 0.077$  and  $\tau = 45s$

given by eqn. (3) and the fluxes for other species can be computed from eqn. (3), the reaction mechanism and the stoichiometric eqn. (1). The solution of eqns. (14) and (15) were previously described by Mukkavilli et al. [7] in detail. It is noted that Mukkavilli et al. simulated performance of a CFSTR for the cobalt-D2EHPA extraction by employing different drop rate constants ( $C_1, C_2, C_3,$  and  $C_4$ ) than the ones used in this work. Also, the operating conditions ( $\tau = 10s$ ) and physicochemical properties employed in their calculations are not appropriate for our system.

#### EXPERIMENTAL SYSTEM

##### Laser Capillary Spectrophotometer

In order to measure bivariate drop size-concentration distribution data in reactive liquid-liquid dispersions, a laser capillary spectrophotometric (LCS) technique has been developed [8,9].

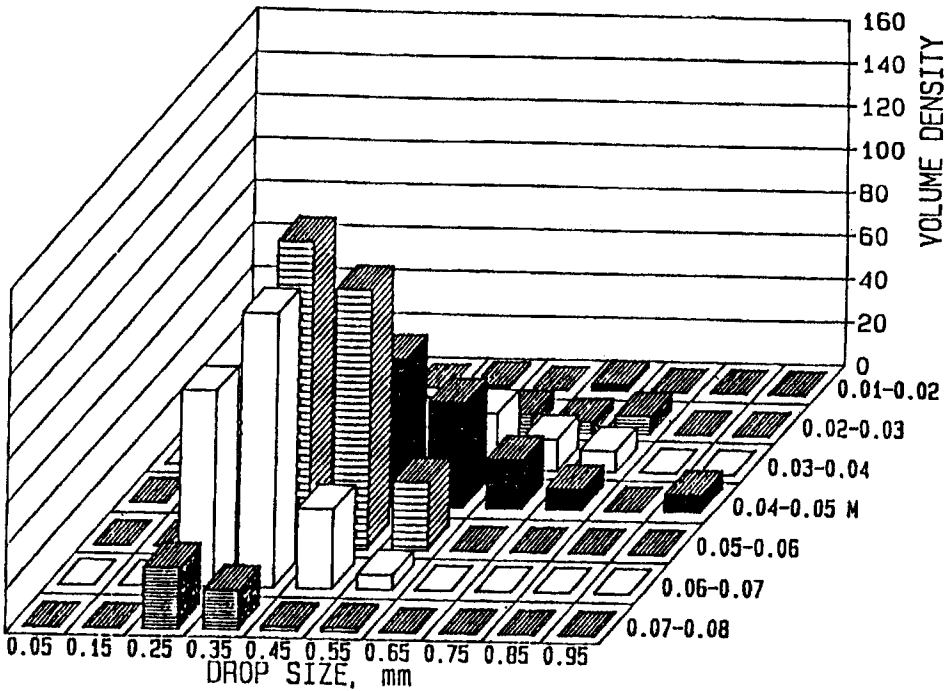


Figure 5: Bivariate Drop Size-Concentration Distribution  
 at  $\phi = 0.077$ ,  $\tau = 45$ s, RPM = 300;  $D_{32} = 0.382$ mm,  
 $C_{av} = 0.0536$ M

This technique is an extension of the capillary sampling method which was tested by Janjua [16] and Blaß and co-workers [17,18] for measurement of drop size.

The variation of the drop size distributions at four different rates of energy dissipation is shown in Figure 3. The figure shows that as the rate of energy dissipation increases from  $0.164 \text{ m}^2/\text{s}^3$  to  $0.673 \text{ m}^2/\text{s}^3$  (or the rotational speed impeller increases 250 RPM to 400 RPM), the marginal drop size distributions become narrower and tend toward the direction of smaller drop sizes resulting in decreased Sauter mean diameters. The figure indicates that the dispersion characteristics are dominated by breakage in the cobalt-D2EHPA extraction system at these high rates of energy dissipation ( $\epsilon = 0.673 \text{ m}^2/\text{s}^3$ ). Drop concentration distributions at four different rates of energy dissipation are shown in Figure 4. The figure indicates that the marginal drop concentration distributions

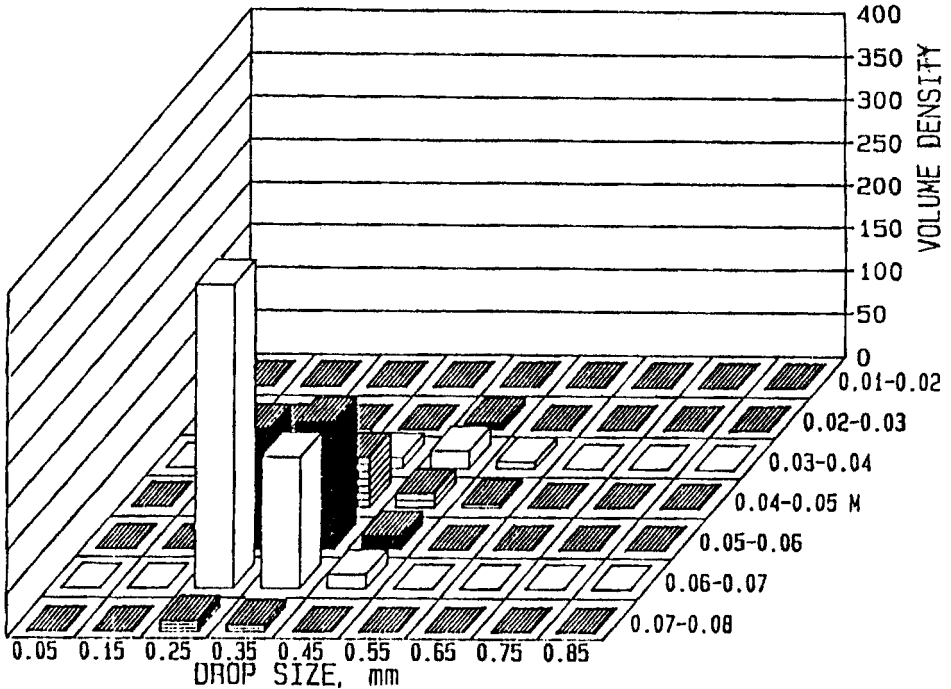


Figure 6: Bivariate Drop Size-Concentration Distribution at  $\phi = 0.077$ ,  $\tau = 45$ s, RPM = 400;  $D_{32} = 0.295$ mm,  $C_{av} = 0.586$ M

become narrow and tend towards higher drop concentrations as the rate of energy dissipation increases. In all cases, however, even at the largest value of RPM (or energy dissipation), there is a broad distribution of cobalt complex concentration.

Bivariate drop size-concentration distributions are shown in Figure 5 for 250 RPM (or  $0.284 \text{ m}^2/\text{s}^3$ ) and in Figure 6 for 400 RPM (or  $0.673 \text{ m}^2/\text{s}^3$ ). These figures illustrate that the bivariate drop size and drop concentration distributions become narrow toward the direction of smaller drop size and larger drop concentration simultaneously as the rotational speed of the impeller increases. It is also noticed that the cobalt concentrations in the drops are widely distributed at low residence time (300 RPM; Figure 5), and perfect mixing of drop concentrations in the dispersed phase should not be assumed at this operation condition. Figure 7 shows the variation of Sauter mean diameter and extrac-

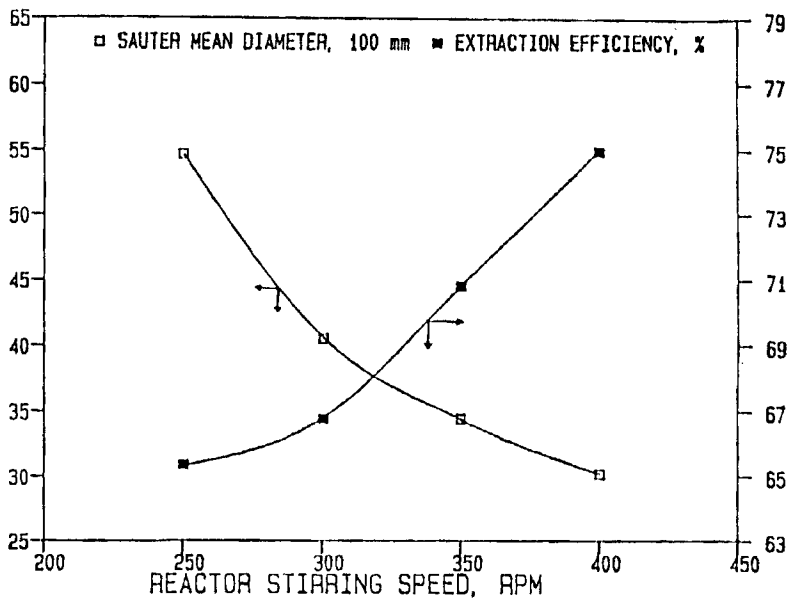


Figure 7: Influence of RPM on  $D_{32}$  and Extraction Efficiency in 1M D2EHPA - 0.01M Cobalt Nitrate at  $\phi = 0.100$  and  $\tau = 45\text{s}$

tion efficiency with rotational speed of the impeller. Extraction efficiency is defined as the ratio of the volume average cobalt complex concentration in the organic phase leaving the reactor to that value if equilibrium were obtained at the feed conditions (fractional approach to equilibrium). As expected, the Sauter mean diameter decreases and extraction efficiency increases as the rotational speed increases from 250 RPM to 400 RPM (or  $\epsilon$  increases  $0.164 \text{ m}^2/\text{s}^3$ ).

#### Comparison of Experimental and Predicted Results

The Monte Carlo simulation method, featuring a stochastic treatment of the interdrop mixing, can predict Sauter mean diameter, drop size distribution and extraction efficiency when the kinetic model of Lee [6] is employed.

Comparisons of Sauter mean diameter between experimental and simulated values versus residence time are depicted in Figure 8. The experimental and simulated Sauter mean diameter are considered to be in reasonably good agreement since the simulation model can

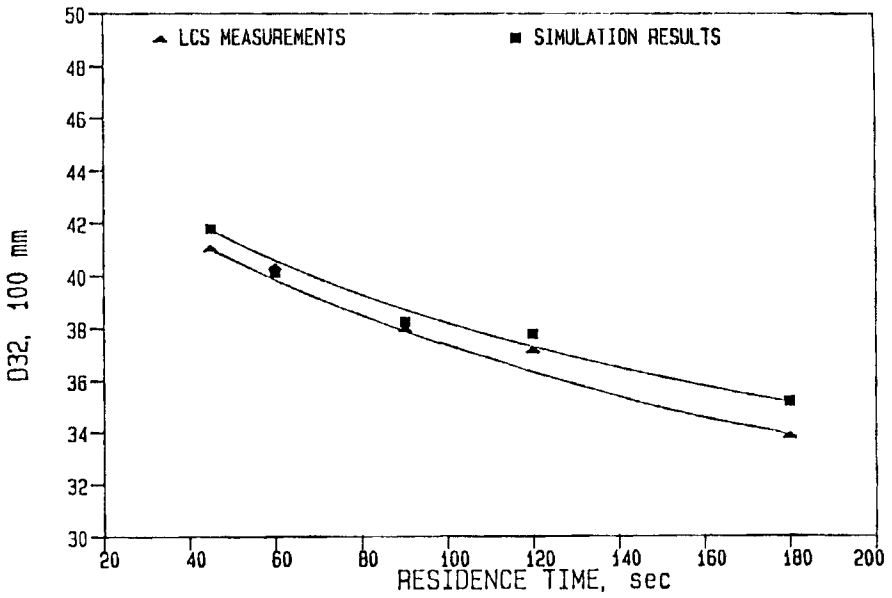


Figure 8: Comparison of  $D_{32}$  with Simulation Results at  $\phi = 0.1$  and RPM = 300

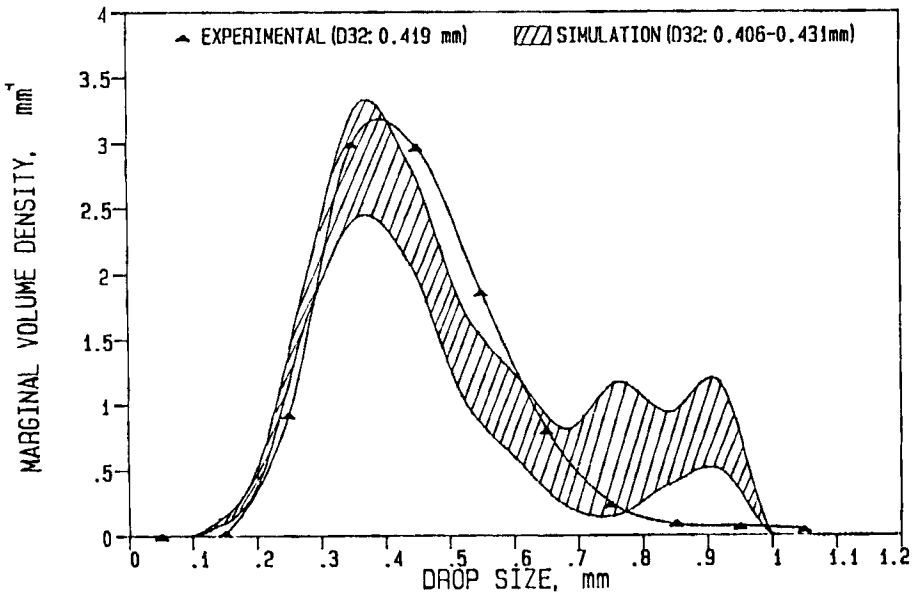


Figure 9: Comparison of Drop Size Distribution with Simulation Results at  $\phi = 0.1$ , RPM = 300 and  $\tau = 45s$

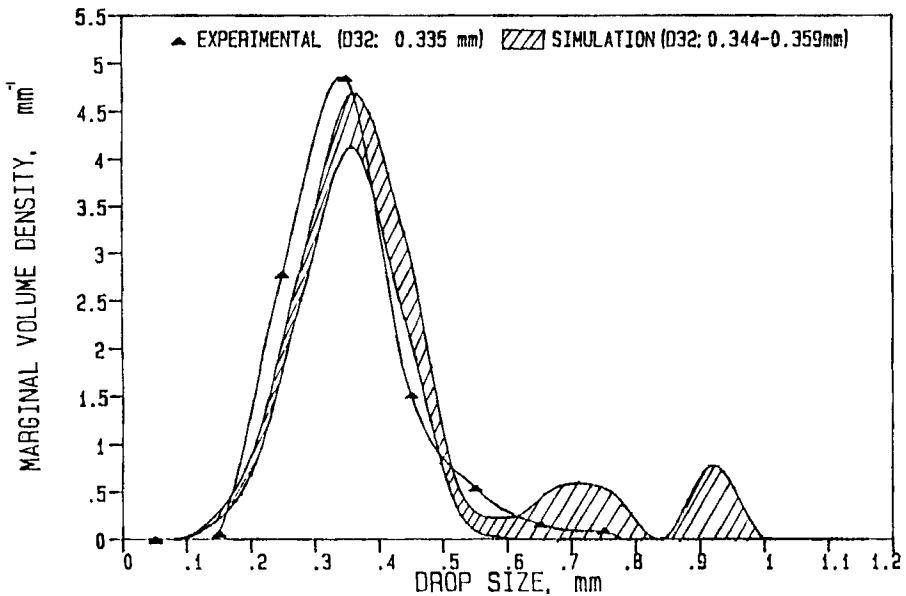


Figure 10: Comparison of Drop Size Distribution with Simulation Results at  $\phi = 0.10$ , RPM = 300 and  $\tau = 150s$

predict Sauter mean diameter within 10% of the experimental values. The predicted drop size distributions and experimental values are compared in Figures 9 and 10. The cross hatched area represents the inherent oscillations in the steady-state simulation results due to the finite size of the sample. The secondary peak at larger drop diameters corresponds to the feed drops. The agreement between the experimental drop size distributions and the predicted values is good at these operating conditions (at operation of  $\tau = 45s$  and  $150s$ ).

Comparison of experimental extraction efficiency with predicted values is shown in Figure 11. The figure shows that the predicted extraction efficiency by the simulation model increases with the residence time, similar to the trend of experimental data, and gives good comparison with measured values, especially above  $\tau = 60sec$ .

It is noted that no adjustable parameters were employed in the model to predict the performance of the one liter flow reactor data. Two separate works were combined for the data analysis



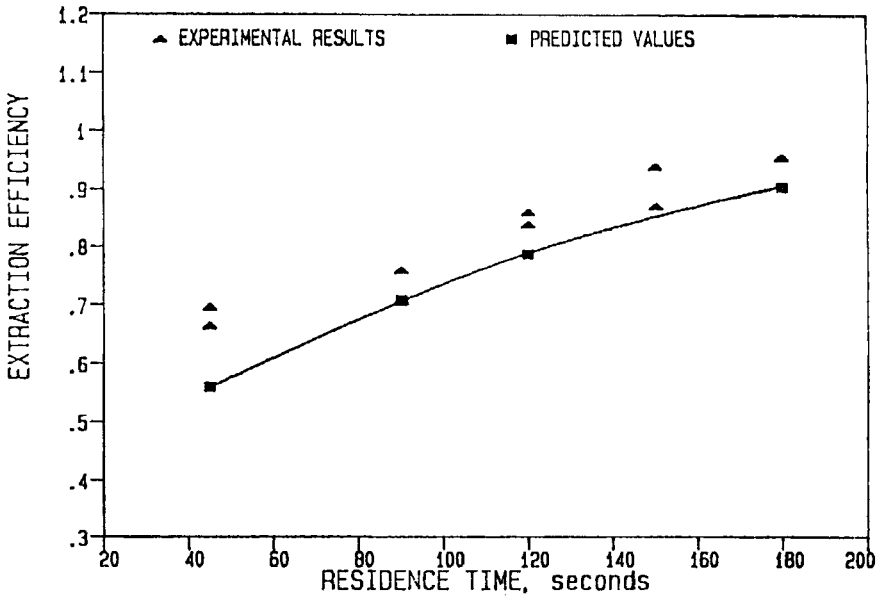


Figure 11: Comparison of Experimental and Predicted Values of Extraction Efficiency Versus Residence Time at  $\phi = 0.1$  and RPM = 300

[6,12], and the parameters of the models were used without change. Accordingly, these results indirectly support the film mechanism employed to describe the cobalt extraction reaction for this system and the Monte Carlo simulation modelling of the liquid dispersion dynamics. Another study reported elsewhere [19,22], compares the film model to the interfacial reaction model for cobalt extraction in detail.

#### CONCLUSION

The laser capillary spectrophotometric (LCS) technique is shown to be capable of producing bivariate drop size-concentration distribution data to study dispersed phase mixing in reacting liquid-liquid dispersions. The extraction of cobalt ions by D2EHPA in toluene in a continuous flow stirred tank can be quantified by the LCS technique, and the influence of the dispersed phase mixing on drop size, drop concentration and extraction efficiency can be described. With the increase of energy dissipation (or RPM), the drop size decreases and drop concentration

(or extraction efficiency) increases. Also, as energy dissipation increases, the drop size distributions become narrow and tend to smaller drop sizes and the concentration distributions become narrow and tend to larger concentrations.

The Monte Carlo simulation algorithm based on the interval of quiescence method can be used to predict Sauter mean diameter, drop size distributions and extraction efficiency. Sauter mean diameter is predicted within 10% of error range and drop size distributions are predicted closely with measured values. The trends in extraction efficiency are also modeled properly with predictions within 15% of measured values.

## NOMENCLATURE

|             |   |
|-------------|---|
| $C_1, C_2$  | constants in the breakage frequency function                |
| $C_3, C_4$  | constants in the coalescence frequency function             |
| $C_{av}$    | average cobalt complex concentration in the dispersed phase |
| CFSTR       | continuous flow stirred tank                                |
| $D_{32}$    | Sauter mean diameter  |
| $d_i$       | diameter of the $i$ th drop                                 |
| D2EHPA      | di-(2-ethylhexyl) phosphoric acid                           |
| $D_i$       | diffusion coefficient of species $i$                        |
| $f_i$       | long range average frequency function of $i$ th event       |
| $F(v, v')$  | coalescence frequency between drops of volume $v$ and $v'$  |
| $g(v)$      | breakage frequency of a drop volume $v$                     |
| $h(v, v')$  | collision frequency between drops of volume $v$ and $v'$    |
| $J_i$       | interfacial flux of species $j$                             |
| LCS         | laser capillary spectrophotometer                           |
| $k_1$       | reaction rate constant, Eq. (2)                             |
| $K_2$       | dissociation constant, Eq. (2)                              |
| $K_A$       | dissociation constant, Eq. (2)                              |
| $K_{ex}$    | association constant, Eq. (1)                               |
| $K_o$       | equilibrium constant, Eq. (2)                               |
| $P_i$       | probability of an event $i$                                 |
| $P_{HR}$    | distribution coefficient for HR, Eq. (3)                    |
| $P_{CoR_2}$ | distribution coefficient for $CoR_2$ , Eq. (3)              |

|          |   |
|----------|---|
| $R_A$    | reaction rate of HR in the aqueous phase        |
| RPM      | rotational speed of the impeller                |
| $t_{IQ}$ | interval of quiescence, defined in Ed. (4)      |
| $v$      | drop volume                                     |
| $V_c$    | continuous phase volume                         |
| $V_d$    | dispersed phase volume of the sample            |
| $V_f$    | average dispersed phase volume of the feed drop |

## Subscript

|   |   |
|---|---|
| b | breakage  |
| c | coalescence   |
| e | exit  |
| f | feed  |
| i | ith drop or interfacial concentration<br>or ith event |
| j | jth species   |
| o | bulk concentration                                    |
| t | total   |

## Superscript

|        |  |
|--------|--|
| d or c | dispersed or continuous phase<br>organic phase species |
|--------|--|

## Greek Letters

|                  |  |
|------------------|--|
| $\delta$         | thickness of aqueous phase film            |
| $\epsilon$       | specific power input or energy dissipation |
| $\theta$         | phase fraction holdup                      |
| $\lambda(v, v')$ | coalescence frequency                      |
| $\mu$            | viscosity                                  |
| $\rho$           | density                                    |
| $\sigma$         | interfacial tension                        |
| $\tau$           | residence time                             |

## ACKNOWLEDGEMENTS

The financial support by the Department of Energy, Office of Basic Sciences, grant number DE-AC02-82ER13002 and partial support

by the Exxon Educational Foundation are gratefully acknowledged. Also, the International Atomic Energy Fellowship provided to one of us (M.S.) is gratefully acknowledged.

## REFERENCES

1. Curl, R. L., *AIChE J.*, 9, 175 (1983).
2. Spielman, L. A. and Levenspiel, O., *Chem. Eng. Sci.*, 20, 247 (1965).
3. Shain, S. A., *AIChE J.*, 12, 806 (1966).
4. Valentas, K. J. and Amundson, N. R., *Ind. Chem. Funda.*, 7, 66 (1968).
5. Zeitlin, M. A. and Tavlarides, L. L., *AIChE J.*, 18, 1268 (1972).
6. Lee, C. K., Ph.D. Thesis, Syracuse University, Syracuse, NY (1986).
7. Mulkavilli, S., Lee, C. K., Hahn, I. and Tavlarides, L. L., *Sep. Sci. and Tech.*, 22 (2&3), 395 (1987).
8. Bae, J. H. and Tavlarides, L. L., submitted to *AIChE J.* (March 1988).
9. Komasaawa, I., Otake, T. and Higaki, Y., *J. Inorg. Nucl. Chem.*, 43, 3351 (1981).
10. Hughes, M. A. and Zhu, T., *Hydrometallurgy*, 13, 249 (1985).
11. Bapat, P. M., Tavlarides, L. L. and Smith, G. W., *Chem. Eng. Sci.*, 38, 2003 (1983).
12. Bapat, P. M. and Tavlarides, L. L., *AIChE J.*, 31, 659 (1985).
13. Smith, G. W., Ph.D. Thesis, Illinois Institute of Technology, Chicago, IL (1985).
14. Coulaloglou, C. A., Ph.D. Thesis, Illinois Institute of Technology, Chicago, IL (1975).
15. Bapat, P. M., Ph.D. Thesis, Illinois Institute of Technology, Chicago, IL (1982).
16. Janjua, D. G., Ph.D. Thesis, University of London, London (1982).

17. Goldman, G. and Blaß, E. CHISA '84, Vol. 14, (1984).
18. Pietsch, W. and Blaß, E., Chem. Eng. Techn., 10, 73 (1987).
19. Bae, J. H., Ph.D. Thesis, Syracuse University, Syracuse, NY (1988).
20. Bonnet, J. C. and Tavlarides, L. L., Ind. and Chem. Eng. Res., 26, 811 (1987).
21. Rod, V., Chem. Eng. J., 20, 131 (1980).
22. Bae, J. H. and Tavlarides, L. L., submitted to AIChE J., (May 1988).